Journal of Earthquake Engineering
Publication details, including instructions for authors and subscription information:
http://www.tandfonline.com/loi/ueqe20

Dimensional Analysis of SDOF Systems Rocking on Inelastic Soil

R. Kourkoulis [a], I. Anastasopoulos [a], F. Gelagoti [a] & P. Kokkali [a]
[a] School of Civil Engineering, National Technical University, Athens, Greece

Version of record first published: 14 Sep 2012.

To cite this article: R. Kourkoulis, I. Anastasopoulos, F. Gelagoti & P. Kokkali (2012): Dimensional Analysis of SDOF Systems Rocking on Inelastic Soil, Journal of Earthquake Engineering, 16:7, 995-1022

To link to this article: http://dx.doi.org/10.1080/13632469.2012.691615

Journal of Earthquake Engineering, 16:995–1022, 2012

ISSN: 1363-2469 print / 1559-808X online
DOI: 10.1080/13632469.2012.691615

Dimensional Analysis of SDOF Systems Rocking on Inelastic Soil

R. KOURKOULIS, I. ANASTASOPOULOS, F. GELAGOTI, and P. KOKKALI

School of Civil Engineering, National Technical University of Athens, Athens, Greece

Aiming to derive results of generalized applicability and provide a generalization framework for future research on the subject, this article performs a dimensional analysis of SDOF systems rocking on compliant soil, taking account of soil inelasticity, foundation uplifting, and P–δ *effects. The effectiveness of the proposed formulation, under static and dynamic conditions, is verified through numerical analyses of self-similar "equivalent" systems. Then, a parametric study is conducted to gain further insights on the key factors affecting the performance, with emphasis on metaplastic ductility and toppling rotation. It is shown that* P–δ *effects may lead to a substantial reduction of (monotonic) moment capacity, especially in the case of slender and heavily loaded structures. Interestingly, this reduction in moment capacity is compensated (to some extent) by an overstrength that develops during cyclic loading. Asymmetric (near-field) seismic excitations tend to produce larger maximum and permanent rotation, compared to symmetric multi-cycle (far-field) excitations, which are critical in terms of settlement. The dimensionless toppling rotation* $\vartheta_{ult}/\vartheta_c$ *(where* ϑ_c *is the toppling rotation of the equivalent rigid block) is shown to be a function of the factor of safety against vertical loads* FS_v *and the slenderness ratio* h/B*. In the case of lightly loaded systems (*$FS_v \rightarrow \infty$*), soil plastification is limited and the metaplastic response approaches that of the equivalent rigid block :* $\vartheta_{ult}/\vartheta_c \rightarrow 1$*. The toppling rotation* $\vartheta_{ult}/\vartheta_c$ *is shown to decrease with* FS_v *:* $\vartheta_{ult}/\vartheta_c \rightarrow 0$ *for* $FS_v \rightarrow 1$*. The role of the* h/B *becomes increasingly important when the response is governed by soil nonlinearity (*$FS_v \rightarrow 1$*). Finally, an approximate simplified "empirical" equation is proposed, correlating* $\vartheta_{ult}/\vartheta_c$ *with* h/B *and* FS_v.

Keywords Dimensional Analysis; SDOF Systems; Soil-Structure Interaction; Toppling Rotation; Ductility

1. Introduction

Over the past 30 years, extensive research has been conducted to derive deeper understanding on the role of *soil–foundation–structure interaction* (*SFSI*) on the seismic performance of structures (e.g., Jennings and Bielak, 1973; Veletsos and Nair, 1975; Kausel and Roesset, 1975; Gazetas, 1983; Tassoulas, 1984; Wong and Luco, 1985; Gazetas, 1991; Gazetas and Mylonakis, 1998). Soil was typically modeled as an idealized visco-elastic material, assuming that the foundation maintains full contact with the supporting soil. Although such an assumption may have appeared reasonable, especially in view of seismic code provisions requiring "elastic" foundation response, recent strong earthquakes have shown that inelastic soil-foundation response may be inevitable. In fact, while for many years the strong motion

Received 6 August 2011; accepted 2 May 2012.
Address correspondence to I. Anastasopoulos, School of Civil Engineering, National Technical University of Athens, Greece; E-mail: ianast@civil.ntua.gr

records from the devastating earthquakes of Northridge (1994) and Kobe (1995), with recorded PGA of the order of 1 g (0.98 g and 0.85 g, respectively) and PGV of the order of 150 cm/s, were believed to constitute the worst-case scenario, the recent March 11, 2011 M_w9.0 Tohoku-oki "mega" earthquake in Japan showed rather dramatically that even stronger acceleration levels of the order of 3 g are possible [Aoi *et al.*, 2011; Furumura *et al.*, 2011]. Most importantly, perhaps, relatively small magnitude seismic episodes may also produce excessively large acceleration levels: the 2004 M_w6.0 Parkfield earthquake is one such example, where the maximum recorded PGA reached 1.8 g accompanied by a PGV of roughly 100 cm/s [Shakal *et al.*, 2006].

Apparently, under such severe seismic shaking the assumption of elastic soil-foundation response cannot be considered realistic. However, recent research suggests that soil–foundation nonlinear response may be beneficial and should be seriously considered in analysis and design (e.g., Paolucci, 1997; Gazetas *et al.*, 2003; Pecker, 2003; Gajan *et al.*, 2005; Mergos and Kawashima, 2007; Pender; 2007; Harden and Hutchinson, 2006; Gajan and Kutter, 2008). Nonlinear foundation behavior may materialize either in the form of *sliding* or *uplifting* of the foundation from the supporting soil when the seismic inertia exceeds its overturning moment capacity, or may involve mobilization of soil bearing capacity. In any of these cases, the finite capacity of the foundation may act as "seismic isolation," limiting the inertia forces transmitted to the above ground system, and hence reducing the dynamic stressing of the superstructure.

To this end, an urgent need is arising to explicitly account for nonlinear SFSI in modern seismic design. Instead of imposing "safe" limits on forces and moments acting on the foundation (as entrenched by current seismic code provisions), the foundation may be designed following performance-based criteria: nonlinear foundation response could be allowed during strong seismic shaking, while ensuring that the developed displacements and rotations will not pose a risk to the structural integrity of the superstructure. So far, a great amount of research has been conducted on the nonlinear response of shallow foundations, comprising *experimental* (e.g. Ticof, 1977; Maugeri *et al.*, 2000; Knappett *et al.*, 2004; Gajan *et al.*, 2005; Bienen *et al.*, 2007; Paolucci *et al.*, 2008; Gajan and Kutter, 2008) and analytical studies, including : (i) finite element (FE) or boundary element approaches, in which both the structure and the foundation soil are modeled together in one single system through an assemblage of finite elements (e.g. Butterfield and Gottardi, 1994; Bransby and Randolph, 1998; Ukritchon *et al.*, 1998; Martin and Houlsby, 2001; Gourvenec and Randolph, 2003; Gazetas and Aposolou, 2004; Gourvenec, 2007); (ii) rigorous plasticity-based macro-element formulations (e.g., Nova and Montrasio, 1991; Paolucci, 1997; Le Pape and Sieffert, 2001; Crémer *et al.*, 2001; Chatzigogos *et al.*, 2009); and (iii) Winkler-based approaches, where the soil is replaced by a series of distributed nonlinear springs and dashpots (e.g., Houlsby *et al.*, 2005; Allotey and El Naggar, 2003; 2007; Raychowdhury and Hutchinson, 2009).

While most of the above studies have focused on nonlinear soil-foundation response, unavoidably drawing relatively little attention to the realistic simulation of the superstructure (typically represented by combined *M-Q-N* loading, or assumed elastic if included in the analysis or in the experiment), recent attempts have been made to model the entire soil–foundation–structure system giving equal attention to the nonlinear behavior of all its components, and the role of geometric nonlinearities (P-δ effects) in determining the "metaplastic" phase of response (i.e., the performance of the system long after reaching its capacity, until complete failure – toppling). Some of these studies include: (a) FE analysis and shaking table testing of idealized bridge piers [Anastasopoulos *et al.*, 2010; Anastasopoulos, 2010]; and (b) centrifuge model testing [Kutter and Wilson, 2006; Chang

et al., 2006] and FE analysis [Gelagoti *et al.*, 2011; Gelagoti *et al.*, 2012; Kourkoulis *et al.*, 2011] of low-rise frame structures.

Aiming to derive results of generalized applicability and to provide a generalization framework for future research on the subject, this article performs a formal dimensional analysis of a single degree of freedom (SDOF) system rocking on compliant soil, accounting for fully inelastic soil response and taking account of geometric nonlinearities (i.e., foundation uplifting and second order effects). The derived formulation is then utilized to shed light on the effect of key factors governing the rocking behavior of SDOF systems rocking on nonlinear soil, such as the slenderness ratio and the factor of safety against vertical (static) loads. The former has been proven to determine the uplifting potential of the system, while the latter defines the mechanism that governs inelastic foundation response (i.e., uplifting or soil yielding).

2. Dimensional Analysis

Dimensional analysis is a mathematical tool that emerges from the existence of physical similarity and reveals the relationships that govern natural phenomena [Langhaar, 1951]. Through dimensional analysis, it is feasible to derive results of generalized applicability and gain deeper understanding of key problem parameters [Makris and Black, 2004a,b; Makris and Psychogios, 2006; Palmeri and Makris, 2008; Karavasilis *et al.*, 2010; Makris and Vassiliou, 2010; Pitilakis and Makris, 2010]. In this article, dimensional analysis is employed to study the static and dynamic response of SDOF systems rocking on inelastic soil (Fig. 1). A typical example of such a system (representative of a bridge pier) is portrayed in Fig. 1a, referring to a "lollipop" structure of height h carrying a concentrated superstructure mass m. The oscillator has a fundamental period T_{str} (assuming fixed-base conditions) and lies on a surface foundation of width B on a clayey soil deposit of depth z, undrained shear strength S_u, shear wave velocity V_s, and density ρ. In the ensuing, a rigorous formulation of the dimensionless terms pertaining to the problem under consideration is attempted, commencing from the simplest case of a rigid block rocking on rigid base, and gradually introducing the additional parameters upon it.

For the simplest case of a rigid block of width $B = 2b$ (where b is the half width of the foundation) and height $H = 2h$ lying on a rigid base (Fig. 1b), the rocking behavior is a function of its geometry, typically expressed through the slenderness ratio $\alpha = tan^{-1}(B/2h)$ [Yim *et al.*, 1980; Makris and Roussos, 2000; Vassiliou and Makris, 2011], and the characteristics of the input seismic excitation which, in case of idealized seismic motions (such as sinusoidal or Ricker pulses), can be described solely through the amplitude a_E and its characteristic frequency f_E [Zhang and Makris, 2001]. Hence, the rotation of the rigid body ϑ may be expressed as:

$$\vartheta = f(B, h, g, a_E, f_E). \tag{1}$$

According to the Vaschy-Buckingham Π-theorem, a dimensionally homogeneous equation involving k variables may be transformed to a function of $k|n$ dimensionless Π-products, where n is the minimum number of reference dimensions necessary for the description of the physical variables.

Applying the Π-theorem on Eq. (1), which contains $k = 6$ independent variables involving $n = 2$ reference dimensions, obviously results in 4 dimensionless Π-products. In this context, Eq. (1) may be rearranged in dimensionless terms so that:

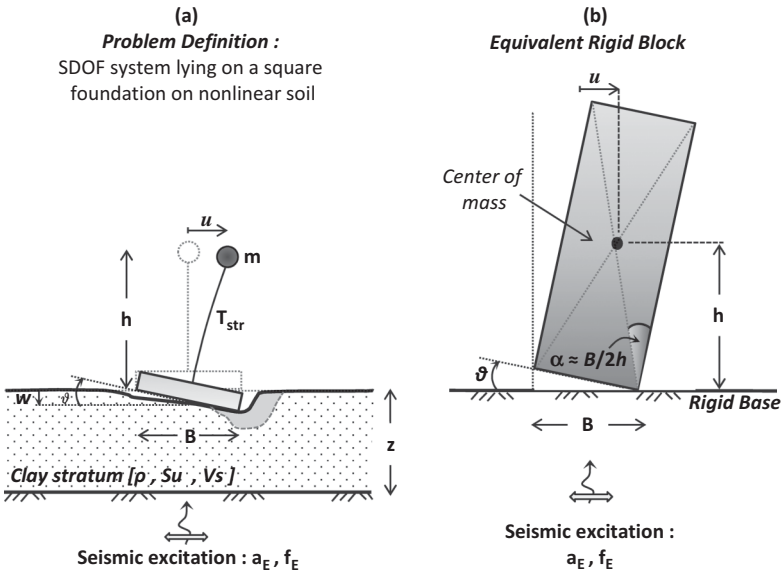

FIGURE 1 Problem definition: (a) SDOF system lying on a square foundation on compliant nonlinear clayey soil under undrained conditions; and (b) equivalent rigid block on rigid base approximation.

$$\vartheta = f(B/h, f_E/p, a_E/g), \tag{2}$$

where

$$p = \sqrt{3g/4R} \tag{3}$$

is a frequency parameter [Housner, 1964], which is indicative of the dynamic characteristics of the rigid block, playing a crucial role for its rocking response and overturning potential. In Eq. (3), R is the half-diameter of the block:

$$R = \sqrt{(B/2)^2 + h^2}. \tag{4}$$

To render Eq. (1) applicable to the general case of a SDOF system rocking on inelastic soil (Fig. 1a), the characteristics of the soil and the superstructure need to be taken into account. This is accomplished by introducing in the equation the fundamental period of the soil and the structure, T_{soil} and T_{str}, respectively, and the soil strength, expressed (for the problem investigated herein) through the undrained shear strength S_u. Lastly, in order to account for kinematic soil response and wave propagation effects, Eq. (1) should also include the depth z, density ρ, and shear wave velocity V_s of the clayey soil layer. Incorporating all of the above in Eq. (1) yields:

$$\vartheta = f(B, h, g, a_E, f_E, T_{str}, m, S_u, z, \rho, V_s) \tag{5}$$

which apparently contains $k = 12$ independent variables involving $n = 3$ reference dimensions (i.e., length, mass, and time). Following the same principles as before, Eq. (5) is re-written in non dimensional terms:

$$\vartheta = f\left(\frac{h}{B},\ \frac{a_E}{g},\ \frac{f_E}{p},\ pT_{str},\ \frac{V_s}{pz},\ \frac{mg}{S_u B^2},\ \frac{\rho V_s^2}{S_u},\ \frac{S_u}{\rho z a_E}\right). \tag{6}$$

The parameter $mg/S_u B^2$ is directly proportional to the ratio $x = N/N_{ult}$ of the static vertical load N of the superstructure to the bearing capacity $N_{ult} = (\pi + 3)\, S_u B^2$ of the square foundation (i.e., the inverse of the factor of safety against vertical loads FS_v); in the sequel, it will be referred to as $1/FS_v$ or $x = N/N_{ult}$. The flexibility of the oscillator is expressed through the oscillator flexibility parameter pT_{str}. Accordingly, soil nonlinearity is expressed through the term $r = S_u/\rho z\, \alpha_E$, in which S_u is the available undrained shear strength, and $\rho z \alpha_E$ is an index of the earthquake-induced stress at depth z. In other words, r may be considered as an index of the mobilization of soil shear strength due to the imposed acceleration α_E . Finally, the factor $v = \rho V_s^2/S_u$ termed "rigidity ratio" in soil mechanics literature, is the ratio of the soil shear modulus (at small strains) over the undrained shear strength. Evidently, at least in its present form, this dimensional analysis is not capable of capturing the effect of excitation type (i.e., number of strong motion cycles, kinematic characteristics, etc.) as it only integrates the peak amplitude $\alpha_E$and characteristic frequency $f_E$of seismic shaking.

According to the presented formulation, the dimensionless settlement and moment of the foundation may be expressed as:

$$\frac{w}{B} = f\left(pt,\ \frac{h}{B},\ \frac{1}{FS_v},\ pT_{str},\ \frac{\rho V_s^2}{S_u},\ \frac{S_u}{\rho z a_E},\ \frac{V_s}{pz},\ \frac{a_E}{g},\ \frac{f_E}{p}\right) \tag{7}$$

$$\frac{M}{S_u B^3} = f\left(\frac{\vartheta}{\vartheta_c},\ \frac{h}{B},\ \frac{1}{FS_v},\ pT_{str},\ \frac{\rho V_s^2}{S_u},\ \frac{S_u}{\rho z a_E},\ \frac{V_s}{pz},\ \frac{a_E}{g},\ \frac{f_E}{p}\right) \tag{8}$$

Table 1 summarizes the independent variables and the dimensionless products of the dimensional analysis for dynamic and static loading.

The ultimate goal of the dimensional analysis presented herein is the production of self-similar results, obeying a special type of symmetry, which is invariant to size (or scale) transformations. In the sequel, the self similarity in the response of example SDOF systems is investigated, by means of nonlinear finite element (FE) analysis, to verify the presented formulation.

TABLE 1 1-DOF systems on surface square foundations subjected to rocking due to static or dynamic loading: Identification of dimensionless Π-products

Independent variables			
$h\ B\ m\ T_{str}\ \rho\ S_u\ V_s\ z$			
Dimensionless products			
Aspect ratio	$\frac{h}{B}$	Rigidity ratio	$\frac{\rho V_s^Z}{S_u}$
Factor of safety	FS_v	Relative frequency	$\frac{V_s}{pz}$
Oscillator flexibility parameter	pT_{Str}	Acceleration amplitude	$\frac{\alpha_E}{g}$
Soil strength mobilization index	$\frac{S_u}{\rho z \alpha_E}$	Frequency parameter	$\frac{J_E}{p}$

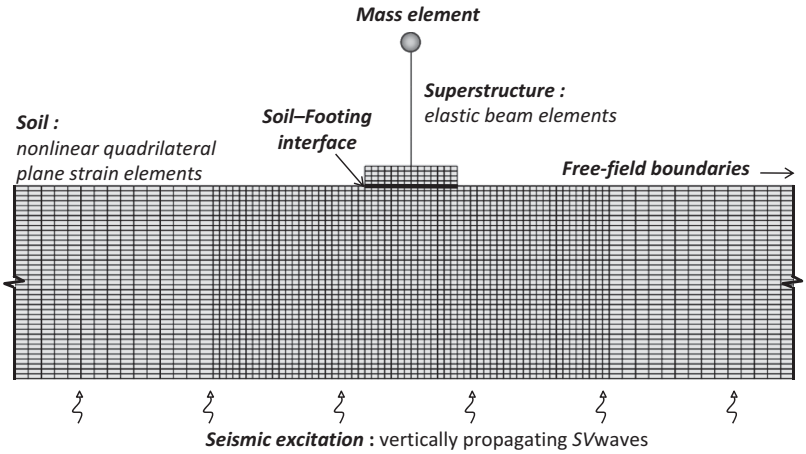

FIGURE 2 Finite element model assuming plane-strain conditions and taking account of material (soil) and geometric nonlinearities (foundation uplifting and P–δ effects).

3. Numerical Analysis Methodology

The FE method is employed in the ensuing in order to confirm the effectiveness of the dimensional formulation and to perform parametric analyses on the effect of each dimensionless term in the rocking behavior of SDOF systems. As depicted in Fig. 2, a "characteristic" slice of the soil–foundation–structure system is modeled considering plane-strain conditions and taking account of material (soil) and geometric (uplifting and P-δ effects) nonlinearities. Quadrilateral continuum elements are used for the soil and the foundation, while the superstructure is modeled with beam elements and a concentrated mass element. The foundation–soil interface is modeled with special contact elements, permitting detachment from the supporting soil.

"*Free-field*" boundaries, materialized through appropriate kinematic constraints, are used at the two lateral boundaries of the model. It is noted that even elementary lateral boundaries placed at an adequately large distance (of the order of 10B) from the footing, would be sufficient for the problem investigated herein, since only a negligible amount of radiation damping is generated thanks to:

(a) the dominant *rocking* mode, due to "destructive interference" of the out-of-phase emitted waves from the two half-sides of the footing [Kausel, 1974];
(b) the fact that the fundamental shear-wave period, T_{soil}, of the soil layer is significantly lower than both the dominant period (T_E) of the earthquake and the natural period (T_{str}) of the superstructure [Kausel, 1974] — especially in view of the fact that the latter increases substantially with uplifting.
(c) the mobilization of the soil yielding and the formation of failure surfaces create a soft zone under the footing, which reflects the incident waves [Borja *et al.*, 1994].

3.1. Soil Modeling

Soil behavior is modeled through a nonlinear kinematic hardening model, with Von Mises failure criterion and associated flow rule [Anastasopoulos *et al.*, 2011]. The evolution law of the model consists of two components: a nonlinear kinematic hardening component, which describes the translation of the yield surface in the stress space (defined through the

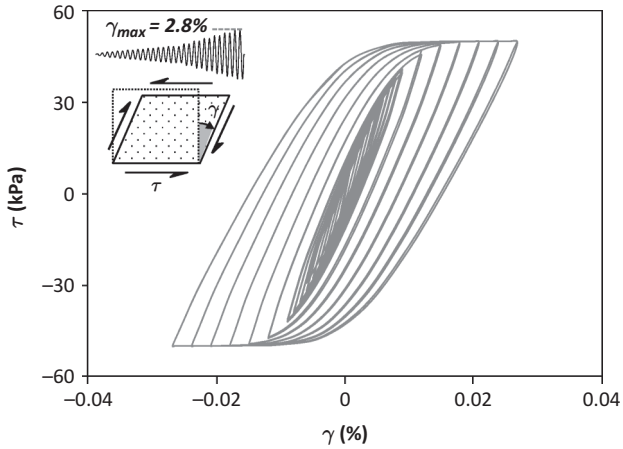

FIGURE 3 Soil Constitutive model: example of model predicted shear stress – shear strain (τ–γ) loop for a single soil element (of undrained shear strength $S_u = 50$ kPa) subjected to cyclic simple shear loading of gradually increasing amplitude.

"backstress" parameter β), and an isotropic hardening component, which defines the size of the yield surface $\sigma_o$as a function of plastic deformation. The pressure-independent yield surface of the model according to the Von Mises failure criterion is defined through the following function F:

$$F = f(\sigma - \beta) - \sigma_0. \tag{9}$$

Calibration of model parameters requires knowledge of: (a) soil undrained shear strength S_u; (b) small-strain stiffness (expressed through G_o or V_s); and (c) stiffness degradation (G–γ and $\xi-\gamma$ curves). Figure 3 plots an example of model predicted shear stress–shear strain (τ–γ) loop for a single soil element (of undrained shear strength $S_u = 50$ kPa) subjected to cyclic simple loading of gradually increasing amplitude. More details on model calibration and comparisons of model predictions in terms of G–γ and ξ–γ curves against published experimental data can be found in Anastasopoulos *et al.* [2011b].

The model is subjected to static and dynamic time-history analysis. In the first case, three different loading types are applied: (i) vertical "push-down" analysis (to estimate the bearing capacity of the foundation); (ii) displacement-controlled monotonic pushover analysis; and (iii) displacement-controlled cyclic pushover analysis. In the latter case (dynamic analysis), the seismic excitation (idealized wavelets and real records), is imposed at the base of the model.

3.2. Equivalence between 2D and 3D FE Models

As previously discussed, a two-dimensional (2D) analysis is conducted, considering a representative "*equivalent slice*" of the soil−foundation–structure system. In order to achieve equivalence between the 2D and the square 3D problem, the Meyerhof [1963] and Vesic [1973] bearing capacity shape factor of 1.2 (for a square foundation) is applied to the out of plane dimension of the soil "slice," following the methodology proposed by Gelagoti *et al.* [2011]. As will be shown in the sequel, this procedure is quite effective in capturing

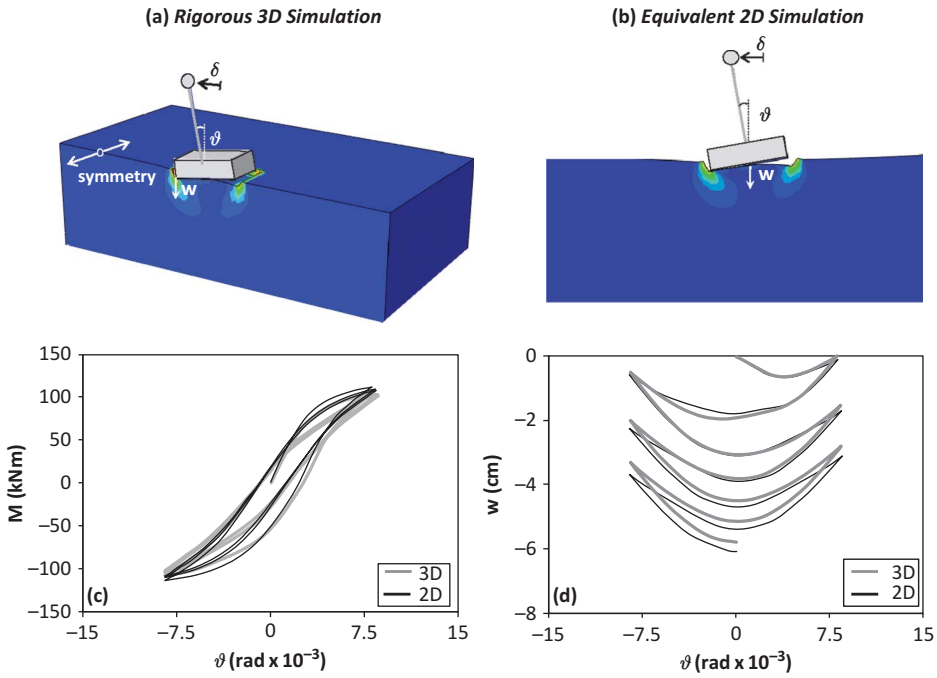

FIGURE 4 Comparison of: (a) rigorous 3D numerical simulation with (b) "equivalent" 2D analysis (deformed meshes with superimposed plastic strain contours). Illustration of equivalence in terms of: (c) moment–rotation (M–ϑ) response and (d) settlement–rotation (w–ϑ) response of a square $B = 1.7$ m footing founded on $S_u = 50$ kPa medium-soft clay (color figure available online).

the nonlinear response of the foundation, but less accurate in terms of the elastic (i.e., small strain) stiffness of the foundation.

In order to demonstrate the validity of this procedure, two FE models were developed to simulate the response of a SDOF system subjected to cyclic pushover loading: a rigorous 3D model (Fig. 4a), and an equivalent *2D* model (Fig. 4b). The specific example refers to a system carrying a superstructure dead load $N = 150$ kN, founded on a square $B = 1.7$ m footing on $S_u = 50$ kPa medium-soft clay. Figures 4c and d compare the two models in terms of moment−rotation ($M-\vartheta$) and settlement−rotation ($w-\vartheta$) foundation response. It is shown that, overall, the equivalent 2D approach reproduces the key aspects of the 3D problem quite effectively, and is hence adopted for the subsequent parametric analyses.

3.3. Validation of FE Analysis Methodology

The FE analysis methodology technique employed herein has been validated [Anastasopoulos *et al.*, 2011] against centrifuge model tests conducted at UC Davis [Kutter *et al.*, 2003; Gajan *et al.*, 2005]. One such comparison is portrayed in Fig. 5, referring to a SDOF system founded on a rectangular foundation, having $FS_v = 2.6$, on layer of remolded San Francisco Bay mud (consolidated on top of a dense sand layer). The tests were conducted at 20 g centrifugal acceleration, applying displacement in packets of increasing amplitude (each containing three cycles of constant amplitude). The comparison shown

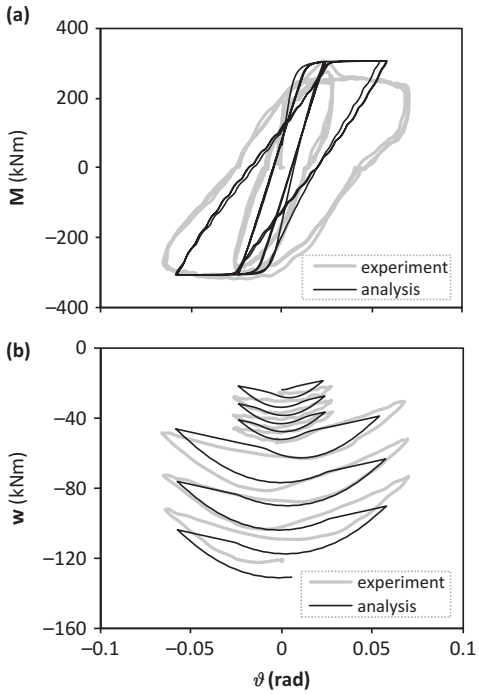

FIGURE 5 Validation of FE analysis and soil constitutive model against UC Davis centrifuge model tests [Kutter *et al.*, 2003] – cyclic loading of a rectangular foundation having $FS_v = 2.6$, resting on remolded San Francisco Bay mud (third loading packet). Comparison of FE analysis with experimental results in terms of: (a) moment–rotation (M–ϑ) and (b) settlement–rotation (w–ϑ) response.

herein refers to the third packet of loading, of maximum rotation amplitude $\vartheta \approx 0.06$ rad. The model predicts correctly the ultimate moment capacity of the footing $M_{ult} \approx 300$ kNm (Fig. 5a), and the accumulation of permanent settlement underneath the footing (Fig. 5b). The non symmetric behaviour (different M_{ult} for the two loading directions), possibly associated to some experimental asymmetry or soil inhomogeneity, cannot possibly be captured by the numerical simulation. The hysteresis loops reveal highly nonlinear response, characterized be excessive soil plastification. Although the total settlement is accurately predicted, as evidenced by the shape of the M–ϑ loops energy dissipation is under-predicted by the model, being associated with an under-prediction of foundation uplifting.

The model is further validated herein against published failure envelopes for surface foundations subjected to combined M-Q-N loading [Butterfield and Gottardi, 1994; Paolluci and Pecker, 1997; Gourvenec, 2007]. One such comparison against the failure envelopes of Gourvenec [2007] is portrayed in Fig. 6, referring to an $h/B = 2$ SDOF system ignoring P–δ effects (to produce compatible results). The plot presents the normalized foundation moment capacity M_{ult}/M_{max} (where M_{ult} is the ultimate capacity of the foundation for the specific vertical load, and M_{max} is the maximum ultimate moment capacity) as a function of the normalized vertical load $x = N/N_{ult}$ $(= 1/FS_v)$. This quite satisfactory comparison reveals the validity of the *equivalent* 2D analysis methodology. Ignoring P–δ effects, the moment capacity of the foundation is maximized for a critical value of $x = 0.5$ (i.e., for a safety factor against vertical loads $FS_v = 2$).

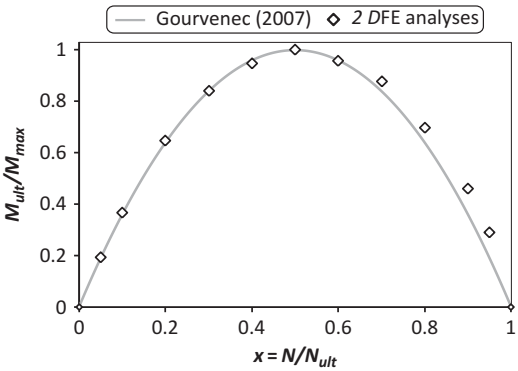

FIGURE 6 Comparison of equivalent 2D FE analysis with the published failure envelope of Gourvenec [2007] for an $h/B = 2$ SDOF system subjected to combined *M-Q-N* loading, ignoring *P–δ* effects: normalized moment capacity M_{ult}/M_{max} as a function.

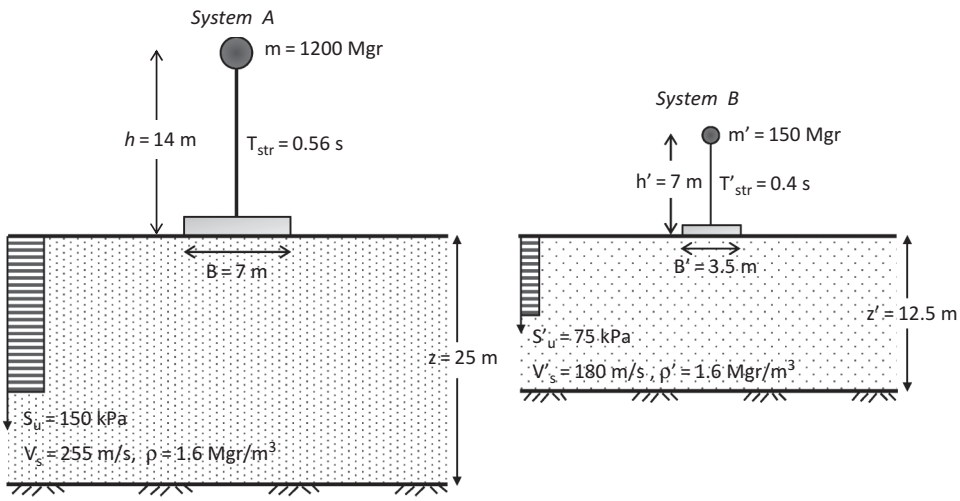

FIGURE 7 Example problem: two unique systems may display a self-similar response as long as they share common dimensionless properties [case study: $h/B = 2$, $FS_V = 2.5$, $pT_{str} = 0.4$, $\rho V_S^2 / S_u = 690$, $V_S / pz = 14.3$].

4. Effectiveness of the Dimensional Formulation

In an attempt to demonstrate the effectiveness of the dimensional analysis described above, this section compares the response of the two *"equivalent" SDOF* systems of Fig. 7, first subjected to monotonic pushover loading (static analysis), and then to strong seismic shaking (dynamic time-history analysis). System A refers to an $h/B = 2$ structure carrying a mass $m = 1200$ Mgr, founded on a $B = 7$ m footing on $S_u = 150$ kPa soil of depth z = 25 m. System B refers to an equivalent structure, founded on a $B' = 3.5$ m footing on $S'_u = 75$ kPa soil of depth z = 12.5 m. Since the FS_v of the two systems must be equal, the mass of *System B* is calculated as $m' = m/8 = 150$ Mgr (since N_{ult} is proportional to B^3). Apparently, the slenderness ratio $h/B = 2$ is common for both systems. Proper adjustment of the shear wave velocity of *System B*, allows the two systems to share the same soil stiffness ratio $\rho V_s^2 / S_u = 690$. The parameter pT_{str} that reflects the flexibility of the oscillators

is equal to 0.34, while the parameter V_s/pz, which is indicative of the relative frequency of the soil-superstructure system, is equal to 14.3.

4.1. Static Pushover Loading

The moment-rotation response of the two systems subjected to static pushover loading is depicted in Fig. 8. As expected, in absolute terms (Fig. 8a) the moment capacity M_{ult} of the two systems is substantially different. The equivalent rigid block of each system represents the upper-bound, both in terms of moment capacity and toppling rotation ϑ_{ult}. In both cases, soil compliance reduces the moment capacity but has a minimal effect on the toppling rotation. Observe that the latter (i.e., ϑ_{ult}) is the same for the two systems, since both share the same slenderness ratio $h/B = 2$ (or $H/B = 4$ in terms of the equivalent

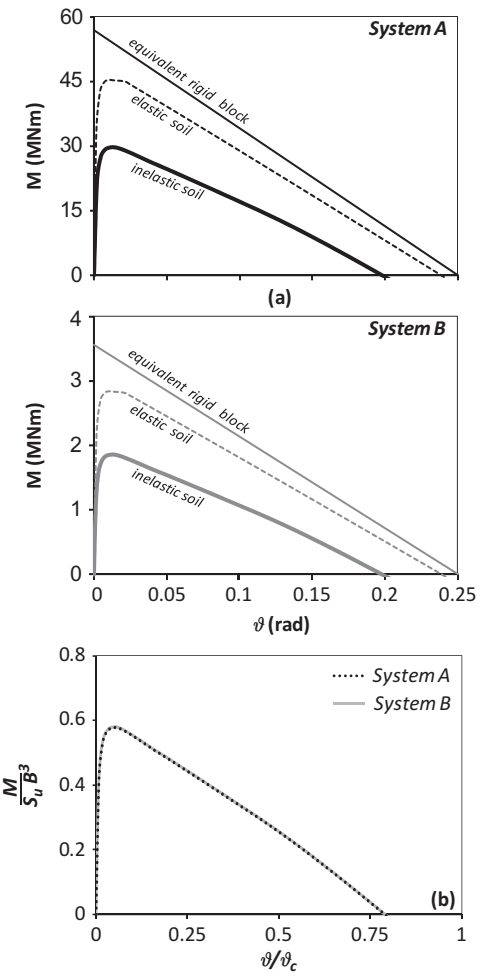

FIGURE 8 Effectiveness of dimensional formulation for static pushover loading. (a) Moment–rotation (M–ϑ) response of the two equivalent systems. The response of the fully nonlinear system is compared to the case of elastic soil, and to the equivalent rigid block on rigid base. (b) Comparison of the two systems in terms of dimensionless moment–rotation response.

rigid block). Accounting for soil inelasticity leads to a substantial reduction of M_{ult} and ϑ_{ult} for both systems. All the above discrepancies fade away once the results are plotted in non dimensional terms (Fig. 8b), confirming the effectiveness of the presented dimensional formulation for static loading. The latter has been confirmed through analyses of various equivalent systems subjected to monotonic and cyclic loading, not shown herein for the sake of brevity.

4.2. Dynamic Loading: Seismic Shaking

The equivalence of the two systems subjected to seismic shaking has been verified through nonlinear dynamic time history analyses, using as seismic excitation idealized (Ricker and sinusoidal) pulses and an ensemble of 18 strong motion records (see Gelagoti *et al.*, 2011), covering a wide range of seismic scenarios. An example comparison is depicted in Fig. 9, which refers to the nonlinear dynamic time history analysis of the two systems, applying as seismic excitation the Takatori (000) accelerogram, which was recorded during the devastating 1995 Kobe earthquake. This record constitutes a rather devastating seismic excitation, characterized by forward rupture directivity effects, large number of strong motion cycles, and PGV of the order of 150 cm/s. It is used to test the effectiveness of the dimensional formulation under extremely nonlinear conditions.

Quite remarkably, the comparison is excellent both in terms of dimensionless acceleration and settlement time histories, and with respect to dimensionless moment–rotation loops. The dimensionless acceleration time histories at the oscillator mass (Fig. 9a) are practically identical, exhibiting exactly the same dimensionless frequency content. Observe that the maximum acceleration at the oscillator mass is significantly lower than the peak acceleration of the seismic excitation, revealing that the foundations of both systems reached their moment capacity. Extensive soil yielding underneath the footing takes place in both cases, resulting in limiting the inertia transmitted onto the superstructure. The latter is due to the low $FS_v = 2.5$ of the two equivalent systems, which produces substantial accumulation of settlement during each loading cycle (Fig. 9b). Despite such extensive soil yielding, the dimensionless settlement time histories of the two systems are practically identical. Minor discrepancies are observed when comparing the dimensionless moment-rotation loops of the two equivalent systems (Fig. 9c).

In summary, the presented dimensional formulation facilitates the derivation of results of generalized validity for the fully nonlinear problem under static and dynamic loading taking account of soil inelasticity, uplifting, and second-order effects. It is emphasized that the presented formulation is equally successful for the entire range of response: from quasi-elastic conditions (i.e., for very small imposed rotation) until toppling.

5. Parametric Analysis and Further Insights

The following sections investigate the effect of key dimensionless parameters on the rocking response of SDOF systems rocking on inelastic soil. Exploiting the proposed dimensional formulation, parametric analysis results are presented in dimensionless terms, thus corresponding to a "family" of equivalent systems rather than individual cases.

5.1. The Effect of Static Safety Factor FS_V

Two pairs of equivalent systems are examined (Table 2), both of aspect ratio $h/B = 2$. The first pair has a factor of safety against vertical loads $FS_v = 2$, thus representing heavily loaded systems, whereas the second pair has $FS_v = 5$, being representative of relatively

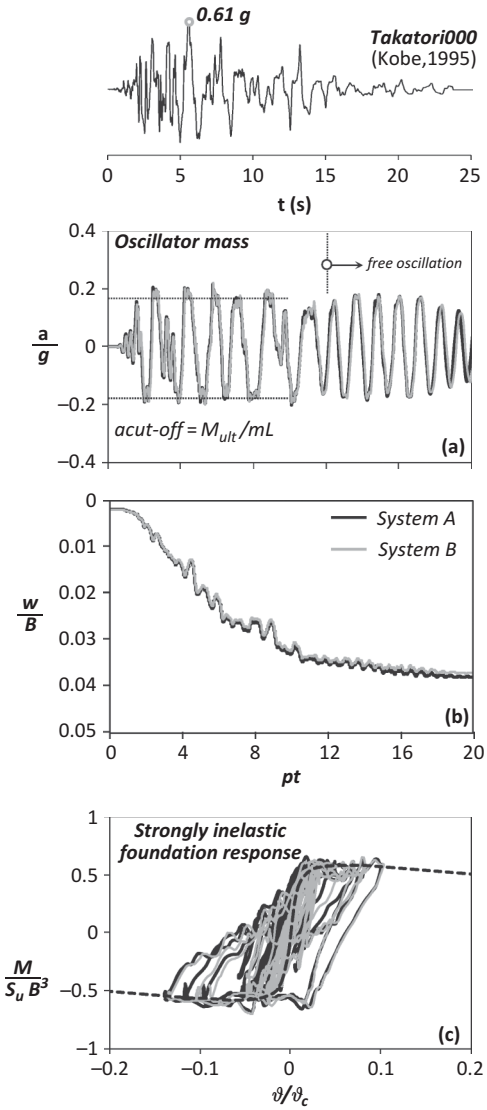

FIGURE 9 Effectiveness of dimensional formulation for strong seismic shaking – nonlinear dynamic time history analysis applying as seismic excitation the Takatori record (Kobe 1955). Dimensionless time histories of: (a) acceleration at the oscillator mass; (b) foundation settlement; and (c) dimensionless moment–rotation loops at the foundation level.

lightly loaded systems. Since the dimensionless response of each pair of systems is identical, in the ensuing they will be referred to as heavily loaded and lightly loaded systems. The two systems are subjected to monotonic and cyclic pushover loading (static analysis), and their performance is comparatively assessed in Fig. 10.

Not surprisingly, FS_v plays a key role in the rocking response of the two systems. As evidenced by the plastic strain contours of Fig. 10a (monotonic pushover loading), in the case of the heavily loaded system ($FS_v = 2$) extensive soil plastification takes place underneath the footing, leading to mobilization of a bearing capacity failure mechanism. In effect,

TABLE 2 Independent variables and dimensionless products of two pairs of equivalent systems utilized to illustrate the effect of FS_V. With the exception of FS_V, all dimensionless terms are kept constant. In all cases examined, the superstructure is assumed rigid ($T_{str} \rightarrow \infty$)

Independent variables	Heavily loaded systems				Lightly loaded systems			
	System A		System B		System A		System B	
h (m)	14		7		14		7	
B (m)	7		3.5		7		3.5	
m (Mg)	281	562	38	76	112.5	225	15	30
E (kPa)	90000	180000	45000	90000	90000	180000	45000	90000
S_u (kPa)	75	150	37.5	75	75	150	37.5	75
Dimensionless products								
h/B	2				2			
FS_V	2				5			
E/S_u	1200				1200			

the foundation rotates around pole O', which is shifted to the left of its initial position O (at the center of the footing), i.e., translating opposite to the direction of the imposed rotation. In stark contrast, in the case of the lightly loaded system ($FS_v = 5$), rocking is materialized mainly through uplifting, being accompanied by very limited soil plastification, localized underneath the very edge of the footing. Due to the observed uplifting, the effective width of the foundation decreases substantially, and the rotation pole gradually shifts towards the right edge of the footing (O'').

The dimensionless monotonic moment-rotation response of the two systems is depicted in Fig. 10b. In accord with experimental and analytical findings and published failure envelopes (e.g., Gourvenec, 2007), the heavily loaded $FS_V = 2$ system exhibits greater dimensionless moment capacity compared to the lightly loaded $FS_V = 5$ system. Moreover, as evidenced by the initial inclination of the moment-rotation curve, the "elastic" (small strain) rocking stiffness of the two systems is quite different: the heavily loaded system is characterized by a substantially lower initial stiffness, as a result of initial soil plastification due to the vertical load only. The lightly loaded system topples at a much larger rotation ($\vartheta_{ult}/\vartheta_c \approx 0.9$) compared to the heavily loaded system ($\vartheta_{ult}/\vartheta_c \approx 0.6$), a behavior that conspicuously reflects the increasingly detrimental role of P-δ effects with decreasing FS_v (as explained in detail in the sequel).

The performance of the two systems subjected to cyclic loading of increasing amplitude is summarized in Figs. 10c and d, in terms of dimensionless moment–rotation and settlement–rotation response, respectively (the static backbone curve is also plotted for ease of reference). The shape of the moment-rotation loops of the two systems is quite different: in the case of the heavily loaded $FS_V = 2$ system, the moment-rotation loops are "rounded," contrary to the $FS_V = 5$ system where (at least for large imposed rotation) the loops tend to become "*S-shaped,*" which is indicative of uplifting-dominated response. Interestingly, in this latter case ($FS_V = 5$) the cyclic response is enveloped by the monotonic backbone curve (grey line), while for the heavily loaded system the cyclic moment capacity tends to exceed the monotonic backbone curve: a palpable indication of overstrength. This remarkable feature is probably attributable to soil hardening during repeated cycles of loading, in combination with the role of P–δ effects, as explained in Panagiotidou *et al.* [2012]. In the case of lightly loaded systems (having large FS_V), the rocking response is

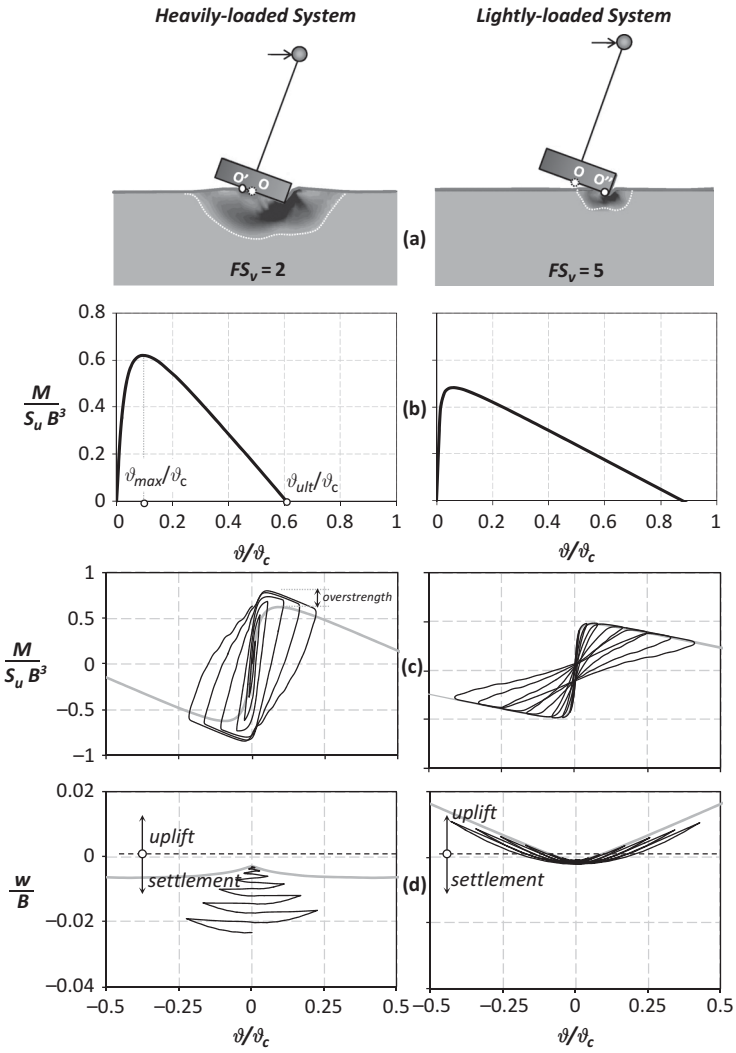

FIGURE 10 Illustration of the effect of FS_v. Comparison of two pairs of equivalent systems subjected to monotonic and cyclic pushover loading, varying only FS_v: (a) deformed mesh with plastic strain contours; (b) dimensionless monotonic moment–rotation response; (c) cyclic dimensionless moment–rotation response; and (d) cyclic dimensionless settlement–rotation response [the grey line corresponds to the monotonic backbone curves].

clearly uplifting-dominated without substantial soil yielding taking place, and the moment capacity is rather a geometric property (almost equals that of the equivalent rigid block, $mgB/2$) leading to the complete absence of such phenomena. This interesting outcome is corroborated by recent experimental studies (e.g., Anastasopoulos *et al.*, 2011).

The qualitatively different response of the two systems is once more evident in terms of dimensionless cyclic settlement-rotation response (Fig. 10d): while the heavily loaded ($FS_V = 2$) system exhibits a sinking-dominated response, accumulating substantial permanent settlement, the lightly loaded ($FS_V = 5$) system tends to uplift, thus developing minor

residual settlement. Noticeably, although the imposed cyclic displacement (at the top of the oscillator) is equal for both systems, the developing rotation is substantially larger for the $FS_V = 5$ uplifting-dominated system compared to the heavily loaded $FS_v = 2$ system. In the former case, the entire imposed displacement is acquired through footing rotation which, in the latter case, is limited due to excessive soil yielding: a substantial portion of the imposed lateral displacement is transformed to horizontal translation at the base of the footing.

5.2. The Role of P–δ effects

Second order P–δ effects are quite invariably neglected in foundation seismic design. The above ground system is typically "represented" by one or more M-Q-N load combinations, based on the static analysis of the superstructure. In the previous section, a first indication of the role of P–δ effects was discussed, shown to be beneficial in terms of the overstrength observed during cyclic loading. However, P–δ effects are not always beneficial. In fact, as it will be shown in the sequel, their role may be detrimental and, hence, neglecting them may lead to unconservative design. To better illustrate such effects, the monotonic pushover response of two pairs of SDOF systems is examined, one referring to a relatively short $h/B = 1$ system and the other to a slender $h/B = 4$ structure. Both systems are analyzed for a variety of superstructure loads, to cover the entire range of $x = N/N_{ult}$ $(= 1/FS_v)$. The characteristics of the self-similar systems analyzed herein are outlined in Table 3. As in the previous section, since the dimensionless response of each pair of systems is identical, in the ensuing they will be referred to as short and slender systems.

The results are summarized in Fig. 11, focusing on the dimensionless failure envelopes of the two systems, ignoring or accounting for P–δ effects. Apparently, P–δ effects are always detrimental in terms of monotonic moment capacity. As shown in Fig. 11a, their effect is minimal for short structures ($h/B = 1$), leading to a maximum decrease of the moment capacity of the order of 5% (observed at $x = N/N_{ult} = 0.6$). In the case of such short structures, the governing failure mechanism tends to be in the form of horizontal translation rather than rotation (i.e., shear failure being critical rather than moment), leading to the observed insensitivity to P–δ effects. In contrast, as the slenderness of the structure

TABLE 3 Independent variables and dimensionless products of two pairs of equivalent systems utilized to illustrate the role of P–δ effects. Two pairs of systems are analyzed, a relatively short system with $h/B = 1$, and a slender system of $h/B = 4$. In all cases examined, the superstructure is assumed rigid ($T_{str} \to \infty$)

Independent variables	Short system				Slender system			
h	1.75		3.5		14		7	
B	1.75		3.5		3.5		1.75	
m	varies parametrically				varies parametrically			
E	45000	90000	90000	180000	45000	90000	90000	180000
S_u	37.5	75	75	150	37.5	75	75	150
Dimensionless products								
h/B	1				4			
X	$0.05 \div 0.95$				$0.05 \div 0.95$			
E/S_u	1200				1200			

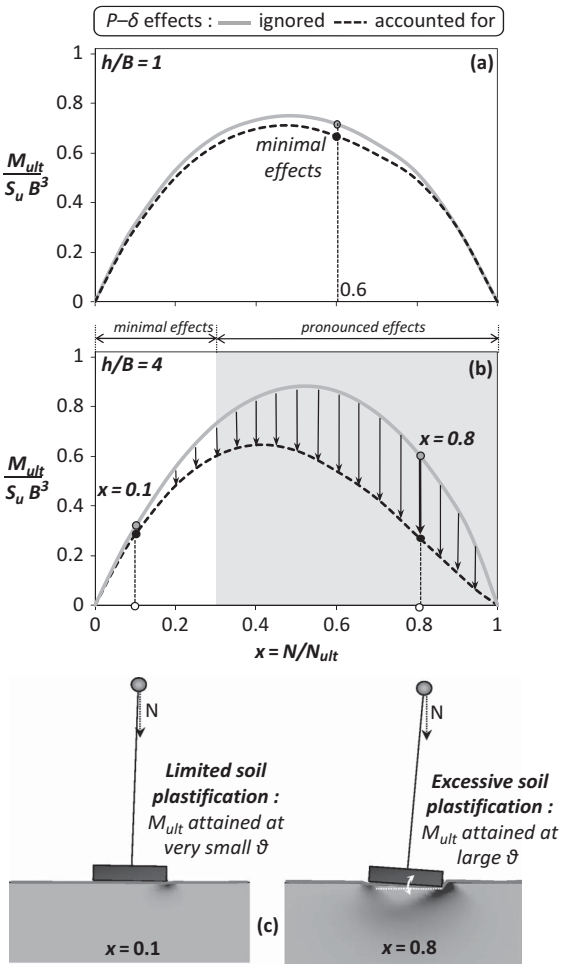

FIGURE 11 Illustration of the role of P–δ effects. Monotonic moment capacity with respect to the dimensionless vertical load $x = N/N_{ult}$ for a pair of equivalent systems: (a) relatively short $h/B = 1$ system, and (b) slender $h/b = 4$ system; (c) schematic explanation of the governing mechanisms for the slender $h/B = 4$ system: deformed mesh with superimposed plastic strain contours at the instant of maximum moment for a lightly loaded ($x = 0.1$) and a heavily loaded ($x = 0.8$) system.

increases ($h/B = 4$), moment becomes the foremost determining factor, and the role of P–δ effects becomes rather pronounced (Fig. 11b). The moment capacity of the system decreases by 20–50% for a wide range of dimensionless load ($0.3 < x < 0.8$). Observe that as $x = N/N_{ult}$ tends to zero (and, hence, FS_v also tends to 1) this decrease in moment capacity due to second-order effects tends to increase even more, exceeding 70%. However, it should be noted that for more realistic values of $x < 0.3$ (i.e., $FS_v > 3.5$) the decrease of moment capacity due to P–δ effects is not that pronounced (i.e., less than 15 %).

A qualitatively explanation of the above is offered by Fig. 11c, which illustrates the plastic strain contours that develop within the soil for the case of the slender $h/B = 4$ system, for two different values of dimensionless vertical load: $x = N/N_{ult} = 0.1$, corresponding to a lightly loaded system, and $x = 0.8$, being representative of a heavily

loaded structure. Both FE snapshots correspond to the rotation at which the maximum foundation moment is attained. In the case of the lightly loaded system (left figure, $x = 0.1$), the failure mechanism is governed by uplifting, not involving substantial soil plastification underneath the footing. As previously discussed, due to such absence of soil plastification, the initial rocking stiffness is close to the elastic and, hence, the moment capacity is attained at a relatively small rotation. As a result, requiring rotation to develop, P–δ effects cannot possibly play an important role. On the contrary, low FS_v systems tend to procure extensive soil yielding underneath them which, in turn, brings about shifting of the pole of rotation away from the center of the footing. Therefore, the moment produced by the superstructure self-weight immediately tends to disturb the system's equilibrium under even low-amplitude rotation. With increasing rotation, the P–δ induced moment is augmented, accelerating the degradation of the moment capacity of the footing.

In summary, P–δ effects may lead to a substantial reduction of the monotonic moment capacity of slender systems, provided that the structure is heavily loaded ($x > 0.3$). Quite interestingly, it is exactly in this case where a substantial cyclic overstrength is observed, also related to P–δ effects. It could be argued that the same mechanism is largely responsible for both phenomena. In fact, it seems that the detrimental role of P–δ effects in monotonic loading is reversed when cyclic loading is considered (in terms of the observed overstrength). As a result, the cyclic moment capacity of such systems may very well be very close to the monotonic capacity, ignoring P–δ effects.

5.3. The Role of Seismic Excitation Type

One of the key objectives of the presented dimensional formulation was to obtain self-similar systems, exhibiting equivalent response when subjected to equivalent dynamic loading (i.e., to the same seismic excitation type, properly adjusted in terms of frequency). The primary scope of this section is to highlight the decisive role of excitation type on the dynamic performance of the soil–foundation–structure system.

To this end, two self-similar systems of $FS_V = 2.5$ and $h/B = 2$ are excited by two entirely different idealized seismic motions, sharing the same dimensionless peak acceleration $\alpha_E/g = 0.6$ and dominant frequency $f_E/p = 4.68$ (Fig. 12): (i) a Ricker pulse and (ii) a modified Tsang-type motion. The first is a clearly asymmetric excitation, containing a single coherent large amplitude pulse, accompanied by two smaller amplitude pulses. Despite its simplicity, this mathematical wavelet bears a strong forward-rupture directivity imprint, and thus it has been extensively utilized in seismological studies, to represent near-field seismic motions [Abrahamson, 2000; Mavroeidis and Papageorgiou, 2003; Garini *et al.*, 2011]. On the other hand, the modified Tsang-type excitation is *symmetric*, encompassing a multitude of strong motion pulses that embodies the characteristics of far-field multi-cycle seismic motions.

The comparison is once more performed in terms of dimensionless settlement time histories, and dimensionless settlement–rotation and moment–rotation curves (Fig. 12). Naturally, since the Tsang-type excitation includes multiple strong motion cycles, considerable settlement is accumulated, leading to a permanent settlement almost seven times larger than for the Ricker pulse (Fig. 12a). However, as revealed by the moment-rotation plots of Fig. 12b, owing to the inherent symmetry of the Tsang-type excitation, such excessive settlement is not combined with permanent foundation rotation. This is certainly not the case when the system is subjected to the "asymmetric" Ricker excitation. The main pulse generates excessive unilateral soil yielding (i.e., only on the one side of the foundation), provoking a large-magnitude rotation that may not be recovered during the subsequent lower intensity pulse. Interestingly, although both motions boast the

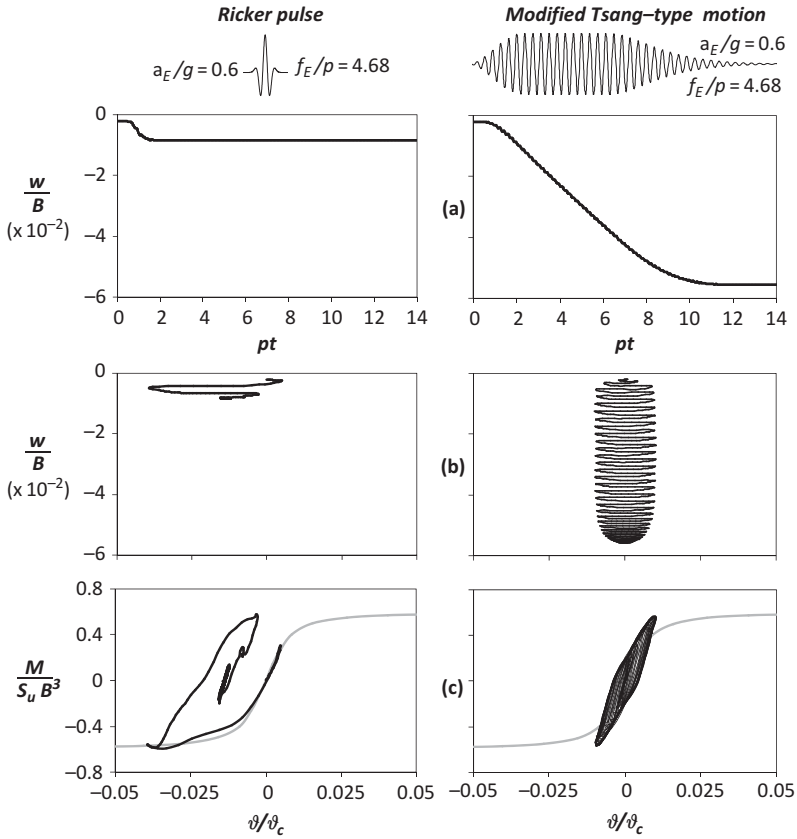

FIGURE 12 Illustration of the effect of excitation type. Nonlinear dynamic analysis of a pair of self similar SDOF systems ($FS_V = 2.5$, $h/B = 2$, $S_u/\rho z\alpha_E = 6.25$), excited by two distinctly different idealized seismic motions: a Ricker wavelet (left column) and a modified Tsang-type motion (right column), sharing the same dimensionless acceleration ($\alpha_E/g = 0.6$) and frequency ($f_E/p = 4.68$): (a) dimensionless settlement time histories, (b) dimensionless moment–rotation, and (c) settlement–rotation response.

same dimensionless acceleration and frequency, the Ricker pulse generates substantially larger maximum rotation $\vartheta_{max}/\ \vartheta_c \approx 0.04$ (compared to less than 0.01 of the Tsang-type excitation).

A plausible explanation is that the Ricker wavelet practically consists of a unique major pulse, immediately generating a significant permanent rotation. On the contrary, the Tsang-type motion consists of a sequence of pulses of the same amplitude, smoothly trailing one another. The produced rotation inevitably follows the same smooth pattern: the rotation acquired during one pulse must be first recovered during the following cycle, and therefore although the Tsang-type excitation boasts the same acceleration amplitude as the Ricker excitation, the developed maximum rotation never actually approaches that of the latter.

The symmetry and monochromatic nature of the Tsang-type excitation is also considered responsible for the observed differences in moment-rotation response (Fig. 12c): although the moment capacity is reached with both excitation types, the moment-rotation loops of the Ricker excitation are much wider, indicating strongly nonlinear foundation

response, something which is not that evident in the case of the multi-cycle Tsang-type excitation.

Further parametric analysis is conducted, using the same idealized seismic motions scaled, but varying the dimensionless acceleration and dominant frequency. The first, α_E/g, is varied from 0.1–1.0 to explore the effects of the mobilized soil nonlinearity. The latter, f_E/p, is parametrically varied from 2.34–4.68, to highlight the role of dimensionless excitation frequency. Figure 13 summarizes the results of the conducted parametric study (referring to $h/B = 2$ systems of $x = 0.4$, i.e., $FS_v = 2.5$), in terms of dimensionless residual and maximum foundation rotation and permanent shaking-induced settlement, with respect to α_E/g and f_E/p.

As expected, all performance measures worsen with the increase of dimensionless acceleration α_E/g. In accordance with the previous discussion, Ricker excitations tend to produce larger rotations, with the multi-cycle Tsang-type motions being critical in terms of permanent settlement. The excitation type clearly plays a major role with respect to the dimensionless maximum rotation (Fig. 13a). Even more important is the

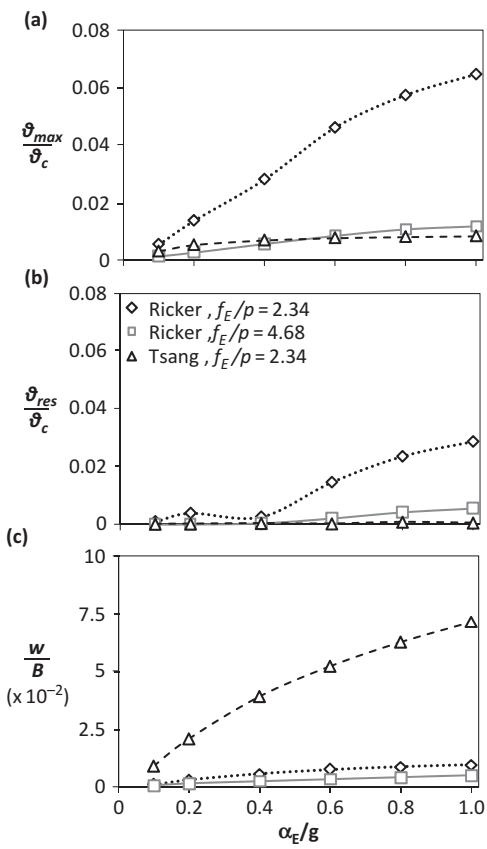

FIGURE 13 Summary of nonlinear dynamic analysis results, referring to self-similar systems of $h/B = 2$ and $FS_V = 2.5$, excited by idealized Ricker and Tsang-type excitations. Performance assessment with respect to dimensionless acceleration α_E/g and dominant frequency f_E/p. Dimensionless: (a) maximum rotation, (b) residual rotation, and (c) settlement.

role of the dimensionless frequency, with the relatively long-period Ricker wavelet of $f_E/p = 2.34$ producing 6 times larger $\vartheta_{max}/\vartheta_c$ compared to its high-frequency counterpart of $f_E/p = 4.68$. The differences are less pronounced when referring to the permanent dimensionless rotation $\vartheta_{res}/\vartheta_c$, but the main trends remain unaltered (Fig. 13b). As expected, the Tsang-type excitation produces substantially larger dimensionless permanent settlement w/B compared to the Ricker pulse of the same frequency content (Fig. 13c). The dimensionless excitation frequency exhibits the same effect: w/B increases with the decrease of f_E/p.

6. Toppling Rotation and Metaplastic Ductility

As previously discussed, a variety of failure envelopes is readily available in the literature for surface foundation subjected to combine *M-Q-N* loading. On the contrary, the "metaplastic" phase of response (i.e., after the ultimate capacity is reached, until toppling) has seldom been given the same attention. As a result, while the strength (i.e., their moment capacity) of rocking systems can be considered to be well known, their ductility is not documented to the same extent. Following the conventional definition of ductility, for a rocking system (assuming elastic superstructure response) it can be defined on the basis of foundation rotation:

$$\mu_R = \vartheta_{ult}/\vartheta_y, \tag{10}$$

where ϑ_{ult} is the toppling rotation and ϑ_y the "yield" rotation. While the exact definition of ϑ_y may be more related to a convention rather than a physical interpretation, ϑ_{ult} represents the absolute limit of the metaplastic response: it signifies the toppling of the system. While the toppling rotation of a rigid block rocking on a rigid base is well known, $\vartheta_c = tan^{-1}(b/h) \approx b/h$, such claim cannot be supported for SDOF systems rocking on inelastic soil.

Hence, exploiting the dimensionless formulation and the key insights of the previously presented parametric analysis, this section attempts to quantify the toppling rotation ϑ_{ult} (which can be used to estimate the ductility μ_R) of foundation–structure systems rocking on compliant inelastic soil. Based on the already presented results, ϑ_{ult} is a function of the h/B ratio and the normalized vertical load $x = N/N_{ult} = 1/FS_v$. A parametric analysis is conducted herein, for h/B ranging from 1–10 (i.e., from short to very slender systems), and covering the entire range of x. Following the structure of the previous sections, ϑ_{ult} is normalized to the toppling rotation ϑ_c of the equivalent rigid block on rigid base. The latter (ϑ_c) is reasonably considered as the upper-bound, and hence when $\vartheta_{ult}/\vartheta_c$ tends to 1 the foundation response is considered to be the most favorable as it approaches the ideal case of rigid block on rigid base. On the other hand, smaller values of $\vartheta_{ult}/\vartheta_c$ suggest poor metaplastic response due to excessive soil yielding.

Figure 14a summarizes the results of the parametric study, plotting $\vartheta_{ult}/\vartheta_c$ as a function of the slenderness ratio h/B and the normalized vertical load $x = N/N_{ult}$. Evidently, for x $\rightarrow$ 0 (i.e., for very large factor of safety $FS_v \rightarrow \infty$), $\vartheta_{ult}/\vartheta_c \rightarrow 1$: due to the extremely light loading acting on the foundation, soil plastification is limited and the response of the system approaches that of the equivalent rigid block. In marked contrast, for x $= N/N_{ult} \rightarrow$ 1 (i.e., for very small $FS_v \rightarrow 1$), $\vartheta_{ult}/\vartheta_c \rightarrow 0$. In this case, the foundation is very heavily loaded, with extensive soil plastification taking place before application of the overturning moment (since $FS_v \rightarrow 1$). Consequently, even the slightest imposed rotation leads to toppling failure, long before the equivalent rigid block. As expected, $\vartheta_{ult}/\vartheta_c$ is also affected by the h/B ratio, the role of which becomes increasingly important as $x \rightarrow 1$, i.e., when the

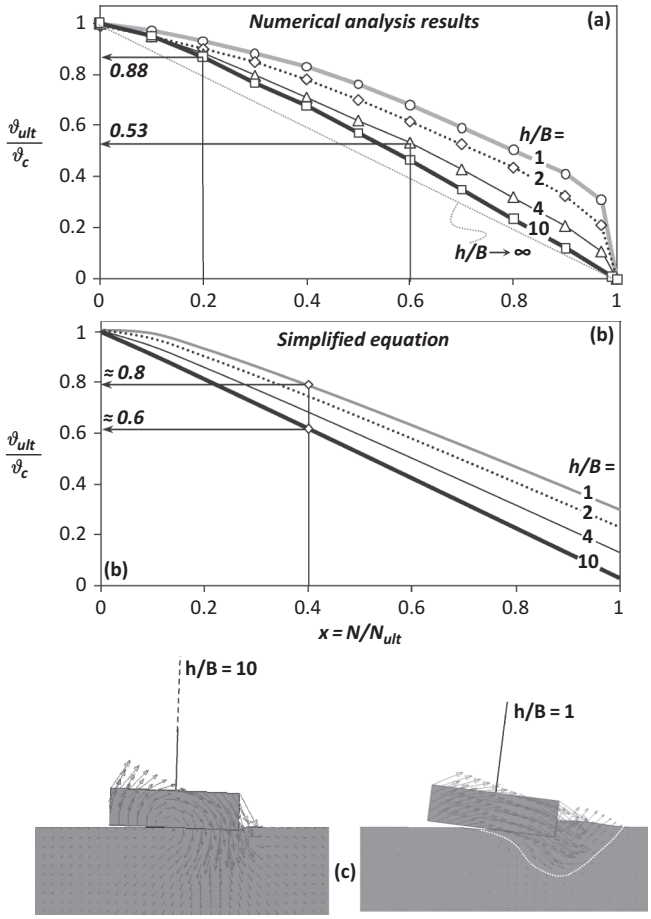

FIGURE 14 Toppling rotation as a function of normalized vertical load x $= N/N_{ult}$ and slenderness ratio h/B: (a) "rigorous" numerical analysis results, compared to (b) proposed simplified approximation. (c) Snapshots of deformed mesh with superimposed displacement vectors for two SDOF systems sharing the same $x = 0.4$, but different h/B ratios.

response is governed by soil nonlinearity. In the opposite case, $x \to 0$, toppling is mainly geometry-related and the role of h/B is minimized.

Based on the presented numerical analysis results, an approximate simplified "empirical" equation is proposed, correlating $\vartheta_{ult}/\vartheta_c$ with h/B and x ($= N/N_{ult}$). Such a correlation may be applied for preliminary estimation of the toppling rotation (and, hence, of the available ductility) of *SDOF* systems rocking on inelastic soil:

$$\frac{\vartheta_{ult}}{\vartheta_c} = (1 - x) + \frac{1}{3}\left[1 - log\left(\frac{h}{B}\right)\right]\sqrt{x}. \tag{11}$$

The proposed equation is graphically illustrated in Fig. 14b to allow for comparison with the "rigorous" numerical analysis solution. Note that the proposed Eq. (11) yields conservative results for the entire range of x and for $1 \leq h/B \leq 10$. Its effectiveness is reduced for

$x < 0.1$ (i.e., for extremely lightly loaded systems) and x > 0.9 (i.e., for extremely heavily loaded systems). For very slender systems, $h/B > 20$, Eq. (11) reduces to:

$$\frac{\vartheta_{ult}}{\vartheta_c} = (1 - x) \tag{12}$$

The previously discussed performance is further elucidated through a numerical example. Let's assume, two slender SDOF $h/B = 4$ systems, the first being lightly loaded ($x = 0.2$) and the second relatively heavily loaded ($x = 0.6$). As already discussed, the dimensionless toppling rotation $\vartheta_{ult}/\vartheta_c$, and hence the rocking ductility μ_R, decreases with increasing $x = N/N_{ult}$ (i.e., with decreasing FS_v) for a given h/B ratio. Indeed, as depicted in Fig. 14a, the metaplastic performance of the lightly loaded system is superior, achieving $\vartheta_{ult}/\vartheta_c = 0.88$ (≈ 0.86 according to the proposed equation), compared to 0.53 ($\approx$ 0.50 according to the proposed equation) of the heavily loaded system. This difference may be attributed to the detrimental role of P–δ effects, which becomes increasingly important for large values of x.

Interestingly, for a given dimensionless vertical load x (i.e., for a given FS_v) the toppling rotation $\vartheta_{ult}/\vartheta_c$ (and hence μ_R) *decreases* with increasing slenderness ratio h/B. An illustrative example is presented in Fig. 14b, referring to two systems carrying the same dimensionless vertical load $x = 0.4$ (i.e., sharing the same $FS_v = 2.5$), but with distinctly different slenderness ratios h/B ratio: a short system of $h/B = 1$, and a very slender system of $h/B = 10$. Evidently, the toppling rotation of the shorter system is substantially larger, reaching $\vartheta_{ult}/\vartheta_c \approx 0.8$ compared to (less than) 0.6 of the slender system. In order to clarify this phenomenon, two deformed mesh snapshots at the instant of maximum moment are presented in Fig. 14c, along with the corresponding displacement vectors. In the case of the slender system (left snapshot), the response of the foundation is governed by the overturning moment leading to a clearly rotational failure mechanism. On the contrary, for low h/B ratios (right snapshot) a "hybrid" failure mechanism is observed, combining rotation and horizontal translation. This failure mechanism seems to be more ductile, as it is accompanied by mobilization of passive failure underneath the front (i.e., right) side of the footing.

7. Synopsis and Conclusions

Aiming to provide a generalization framework for future research on the subject, this paper has presented a formal dimensional analysis of SDOF systems rocking on compliant soil, taking account of soil inelasticity, foundation uplifting, and P–δ (second-order) effects. The effectiveness of the proposed dimensional formulation, under static and dynamic conditions, was verified through numerical analyses of self-similar "equivalent" systems. Then, a parametric study was conducted to gain further insights on the key factors affecting the performance of SDOF systems rocking on nonlinear soil, with emphasis on their metaplastic ductility and toppling rotation.

The main findings of the presented research can be summarized as follows.

1. The factor of safety against vertical loads, FS_v, plays a crucial role in the performance of SDOF system rocking on inelastic soil. In the case of heavily loaded system ($FS_v < 2$) extensive soil plastification takes place underneath the footing, leading to mobilization of a bearing capacity failure mechanism. On the contrary, in the case of lightly loaded systems ($FS_v > 5$) rocking is materialized mainly

through uplifting, with limited soil plastification localized underneath the edge of the footing.

2. Under cyclic loading, a significant overstrength is observed for heavily loaded systems (the cyclic moment capacity exceeds the monotonic backbone curve). This remarkable feature is probably attributable to soil hardening during repeated cycles of loading, in combination with the role of P–δ effects. Being uplifting-dominated, the cyclic response of lightly loaded systems (i.e., having large FS_V) does not exhibit such phenomena: the moment capacity is mainly geometry-related, being almost equals to that of the equivalent rigid block, $mgB/2$. Characterized by sinking-dominated response, heavily loaded systems tend to accumulate substantial permanent settlement. On the contrary, lightly loaded systems exhibit *uplifting*-dominated response, developing minor residual settlements.
3. Second-order (P–δ) effects may lead to a substantial reduction of the monotonic moment capacity, and, hence, neglecting them may lead to unconservative *design*. Their effect is minimal for short structures ($h/B = 1$), where the prevailing failure mechanism is mainly in the form of horizontal translation rather than rotation. For slender structures ($h/B \geq 3$), where moment becomes the prevailing mechanism, P–δ effects become increasingly detrimental leading to a decrease of the monotonic moment capacity of the order of 20–50% for a wide range of dimensionless vertical loads: $0.3 < x < 0.8$ ($x = N/N_{ult} = 1/FS_v$). For more realistic values of $x < 0.3$ (i.e., $FS_v > 3.5$) their role is not that pronounced (leading to a decrease of less than 15%).
4. Quite interestingly, the detrimental role of P–δ effects is observed at the same range of dimensionless vertical load x ($= 1/FS_v$) where a substantial cyclic overstrength is observed, also related to P–δ effects. It may be argued that the detrimental role of P–δ effects in monotonic loading is "reversed" when cyclic loading is considered. Consequently, the cyclic moment capacity of such systems may very well be very close to the monotonic capacity, ignoring P–δ effects — a rather encouraging conclusion, possibly alleviating the risk of unconservative design on the basis of existing failure envelopes (which typically ignore second order effects).
5. Asymmetric Ricker-type excitations, representative of near-field directivity-affected seismic motions, tend produce larger maximum and permanent rotations, compared to symmetric multi-cycle Tsang-type excitations, which are considered representative of far-field seismic motions. The latter, containing multiple strong motion cycles, are critical in terms of permanent settlement. The dimensionless frequency of the seismic excitation f_E/p plays an important role: its *decrease* leads to an increase of maximum and residual rotation and permanent settlement (i.e., long-period motions are more detrimental).
6. The dimensionless toppling rotation $\vartheta_{ult}/\vartheta_c$ (where ϑ_c is the toppling rotation of the equiavlent rigid block on rigid base) of foundation–structure systems rocking on compliant inelastic soil is a function the normalized vertical load $x = N/N_{ult} = 1/FS_v$ and the slenderness ratio h/B. In the case of lightly *loaded* systems (i.e, $x \to 0$; $FS_v \to \infty$), soil plastification is limited and the metaplastic response approaches that of the equivalent rigid block: $\vartheta_{ult}/\vartheta_c \to 1$. Due to increasing soil plastification, $\vartheta_{ult}/\vartheta_c$ decreases with the increase of x (or with the decrease of FS_v): $\vartheta_{ult}/\vartheta_c \to 0$ for $x \to 1$. The role of the slenderness ratio h/B becomes increasingly important when the response is governed by soil nonlinearity ($x \to 1$).
7. An approximate simplified "empirical" equation is proposed, correlating $\vartheta_{ult}/\vartheta_c$ with h/B and x($= N/N_{ult}$), to be applied for preliminary estimation of the toppling rotation of SDOF systems rocking on inelastic soil:

$$\frac{\vartheta_{ult}}{\vartheta_c} = (1 - x) + \frac{1}{3}\left[1 - log\left(\frac{h}{B}\right)\right]\sqrt{x}. \qquad \text{(Eq. 11)}$$

This approximate simplified equation yields conservative results for the entire range of x, and for $1 \leq h/B \leq 10$. Its effectiveness is reduced for $x < 0.1$ and $x > 0.9$. For very slender systems, $h/B > 20$, the following approximation is considered accurate:

$$\frac{\vartheta_{ult}}{\vartheta_c} = (1 - x)\,. \qquad \text{(Eq. 12)}$$

Acknowledgment

The financial support for this article has been provided under the research project "DARE," which is funded through the European Research Council's (ERC) "IDEAS" Programme, in Support of Frontier Research–Advanced Grant, under contract/number ERC–2–9–AdG228254–DARE to Prof. G. Gazetas.

References

Abrahamson, N. A. [2000] "Near-fault ground motions from the 1999 Chi-Chi earthquake," *Proc. of U.S.–Japan Workshop on the Effects of Near-Field Earth Shaking*, San Francisco, March 20–21, pp. 11–13.

Allotey, N. and El Naggar, M. H. [2003] "Analytical moment–rotation curves for rigid foundations based on a Winkler model," *Soil Dynamics and Earthquake Engineering* **23**, 367–381.

Allotey, N. and El Naggar, M. H. [2007] "An investigation into the Winkler modeling of the cyclic response of rigid footings," *Soil Dynamics and Earthquake Engineering* **28**, 44–57.

Anastasopoulos, I. [2010] "Beyond conventional capacity design: towards a new design philosophy," in *Soil–Foundation–Structure Interaction*, eds. R. P. Orense, N. Chouw, and M. J. Pender (CRC Press, Taylor and Francis Group, New York); pp. 213–220.

Anastasopoulos, I., Gazetas, G., Loli, M., Apostolou, M. N., and Gerolymos, N. [2010] "Soil failure can be used for seismic protection of structures," *Bulletin of Earthquake Engineering*, Vol. 8, pp. 309–326.

Anastasopoulos, I., Gelagoti, F., Kourkoulis, R., and Gazetas, G. [2011] "Simplified constitutive model for simulation of cyclic response of shallow foundations: validation against laboratory tests," *Journal of Geotechnical and Geoenvironmental Engineering, ASCE* **137**(2), 1154–1168.

Aoi, S., Kunugi, T., Suzuki, W., Morikawa, N., Nakamura, H., Pulido, N., Shiomi, K., and Fujiwara, H. [2011] "Strong motion characteristics of the 2011 Tohoku-oki earthquake from K-NET and KiK-NET, *SSA Annual Meeting*, Memphis, Tennessee.

Bienen, B., Gaudin, C., and Cassidy, M. J. [2007] "Centrifuge tests of shallow footing behavior on sand under combined vertical-torsional loading," *International Journal of Physical Modeling in Geotechnics* **2**, 1–21.

Borja, R. I., Wu, W. H., Amies, A. P., and Smith, H. A. [1994] "Nonlinear lateral, rocking, and torsional vibration of rigid foundations," *Journal of Geotechnical Engineering, ASCE* **120**(3), 491–513.

Bransby, M. F. and Randolph, M. F. [1998] "Combined loading of skirted foundations," *Géotechnique* **48**(5), 637–655.

Butterfield, R. and Gottardi, G. [1994] "A complete three - dimensional failure envelope for shallow footings on sand," *Géotechnique* **44**(1), 181–184.

Chang, B. J., Raychowdhury, P., Hutchinson, T., Thomas, J., Gajan, S., and Kutter, B. L. [2006] "Centrifuge testing of combined frame-wall-foundation structural systems. *Proc. 8th US National Conference on Earthquake Engineering*, April 18–22, San Francisco, CA, paper No. 998.

Chatzigogos, C. T., Pecker, A., and Salençon, J. [2009] "Macroelement modeling of shallow foundations," *Soil Dynamics and Earthquake Engineering* **29**(5), 765–781.

Crémer, C., Pecker, A., and Davenne, L., [2001] "Cyclic macro-element for soil–structure interaction: material and geometrical nonlinearities," *International Journal for Numerical and Analytical methods in Geomechanics* **25**(12), 1257–1284.

Furumura, T., Takemura, S., Noguchi, S., Takemoto, T., Maeda, T., Iwai, K., and Padhy, S. [2011] "Strong ground motions from the 2011 off-the Pacific-Coast-of-Tohoku, Japan (Mw = 9.0) earthquake obtained from a dense nationwide seismic network," *Landslides* **8**, 333–338.

Gajan, S., Phalen, J. D., Kutter, B. L., Hutchinson, T. C., and Martin, G. [2005] "Centrifuge modeling of load deformation behavior of rocking shallow foundations," *Soil Dynamics and Earthquake Engineering* **25**(7–10), 773–783.

Gajan, S. and Kutter, B. L. [2008] "Capacity, settlement and energy dissipation of shallow footings subjected to rocking," *Journal of Geotechnical and Geoenvironmetal Engineering, ASCE* **134**(8), 1129–1141.

Garini, E., Gazetas, G., and Anastasopoulos, I. [2011] "Asymmetric 'Newmark' sliding caused by motions containing severe 'directivity' and 'fling' pulses," *Géotechnique* **61**(9), 733–756.

Gazetas, G. [1983] "Analysis of machine foundation vibrations: state of the art," *Soil Dynamics and Earthquake Engineering* **2**, 2–42.

Gazetas G. [1991] "Formulas and charts for impedances of surface and embedded foundations," *Journal of Geotechnical Engineering, ASCE* **117**(9), 1363–1381.

Gazetas, G. and Mylonakis, G. (1998] "Seismic soil–structure interaction: new evidence and emerging issues, emerging issues paper," *Geotechnical Special Publications ASCE* (75), 1119–1174.

Gazetas, G. and Apostolou, M. [2004] "Nonlinear soil–structure interaction: foundation uplifting and soil yielding," *Proc. 3rd UJNR Workshop on Soil-Structure Interaction*, Menlo Park, California (available in CD-ROM).

Gazetas, G., Apostolou, M., and Anastasopoulos, I. [2003] "Seismic Uplifting of Foundations on Soft Soil, with examples from Adapazari (Izmit 1999, Earthquake)," *BGA Int. Conf. on Found. Innov., Observations, Design* and *Practice*, Univ. of Dundee, Scotland, September 25, pp. 37–50.

Gelagoti, F., Kourkoulis, R., Anastasopoulos, I., and Gazetas, G. [2011] "Rocking isolation of frame structures founded on separate footings," *Earthquake Engineering and Structural Dynamics* (in print).

Gelagoti, F., Kourkoulis, R., Anastasopoulos, I., and Gazetas, G. [2012] "Rocking isolation of frames on isolated footings: design insights and limitations," *Journal of Earthquake Engineering* **16**(3), 374–400.

Gourvenec S. [2007] "Shape effects on the capacity of rectangular footings under general loading," *Géotechnique* **57**(8), 637–646.

Gourvenec, S. and Randolph, M. F. [2003] "Effect of strength non - homogeneity on the shape and failure envelopes for combined loading of strip and circular foundations on clay," *Géotechnique* **53**(6), 527–533.

Harden, C. and Hutchinson, T. [2006] "Investigation into the effects of foundation uplift on simplified seismic design procedures," *Earthquake Spectra* **22**(3), 663–692.

Houlsby, G. T., Amorosi, A., and Rojas, E. [2005] "Elastic moduli of soils dependent on pressure: a hyperelastic formulation," *Géotechnique* **55**(5), 383–392.

Housner, G. W. (1963] "The behaviour of inverted pendulum structures during earthquake," *Bulletin of the Seismological Society of America* **53**(2), 403–417.

Jennings, P. C. and Bielak, J. (1973) "Dynamics of building-soil interaction," *Bulletin of the Seismological Society of America* **63**(1), 9–48.

Karavasilis, T. L., Makris, N., Bazeos, N., and Beskos, D. E. [2010] "Dimensional response analysis of multi-storey regular steel MRF subjected to pulse-like earthquake ground motions," *Journal of Structural Engineering, ASCE* **136**(8), 921–932.

Kausel, E. (1974] "Forced vibrations of circular foundations on layered media," *M.I.T. Research Report R74-11, Soils Publication No. 336, Structures Publication No. 384*, MIT, Cambridge.

Kausel, E. and Roesset, J. M. (1975] "Dynamic stiffness of circular foundations," *Journal of Engineering Mechanics Division, ASCE* **101**, 771–85.

Knappett, J. A., Haigh, S. K., and Madabhushi, S. P. G. [2006] "Mechanisms of failure for shallow foundations under earthquake loading," *Soil Dynamics and Earthquake Engineering* **26**, 91–102

Kutter, B. L., Martin, G., Hutchinson, T. C., Harden, C., Gajan, S., and Phalen, J. D. [2003] "Status report on study of modeling of nonlinear cyclic load–deformation behavior of shallow foundations," PEER Workshiop, University of California, Davis.

Kutter, B. L. and Wilson, D. L. [2006] "Physical modelling of dynamic behavior of soil-foundation-superstructure systems," *International Journal of Physical Modelling in Geotechnics* **6**(1), 1–12.

Langhaar, H. L. (1951] *Dimensional Analysis and Theory Of Models*, Wiley, New York.

Le Pape, Y. and Sieffert, J. P. [2001] "Application of thermodynamics to the global modelling of shallow foundations on frictional material," *International Journal for Numerical and Analytical Methods in Geomechanics* **25**, 1377–1408.

Makris, N. and Roussos, Y. [2000] "Rocking response of rigid blocks under near-source ground motions," *Géotechnique* **50**(3), 243–262.

Makris, N. and Black, C. J. [2004a] "Dimensional analysis of bilinear oscillators under pulse - type excitations," *Journal of Engineering Mechanics, ASCE* **130**(9), 1019–1031.

Makris, N. and Black, C. J. [2004b] "Dimensional analysis of rigid – plastic and elastoplastic structures under pulse–type excitations," *Journal of Engineering Mechanics, ASCE* **130**(9), 1006–1018.

Makris, N. and Psychogios, T. [2006] "Dimensional response analysis of yielding structures," *Earthquake Engineering and Structural Dynamics* **35**, 1203–1224.

Makris, N. and Vassiliou, M. F. [2010] "The existence of 'complete similarities' in the response of seismic isolated structures subjected to pulse-like ground motions and their implications in analysis," *Earthquake Engineering and Structural Dynamics* **40**(10), 1103–1121.

Martin, C. M. and Houlsby, G. T. [2001] "Combined loading of spudcan foundations on clay: numerical modeling," *Géotechnique* **51**(8), 687–699.

Maugeri, M., Musumeci, G., Novità, D., and Taylor, C. A. [2000] "Shaking table test of failure of a shallow foundation subjected to an eccentric load," *Soil Dynamics and Earthquake Engineering* **20**(5–8), 435–444.

Mavroeidis, G. P. and Papageorgiou, A. S. [2003] "A mathematical representation of near-fault ground motions," *Bulletin of the Seismological Society of America* **93**(3), 1099–1131.

Mergos, P. E. and Kawashima, K. [2005] "Rocking isolation of a typical bridge pier on spread foundation," *Journal of Earthquake Engineering* **9**(2), 395–414.

Meyerhof, G. G. [1963] "Some recent research on the bearing capacity of foundations," *Canadian Geotechnical Journal* **1**(1), 6–26.

Nova, R. and Montrasio, L. [1991] "Settlement of shallow foundations on sand," *Géotechnique* **41**(2), 243–256.

Palmeri, A. and Makris, N. [2008] "Response analysis of rigid structures rocking on a viscoelastic foundation," *Earthquake Engineering and Structural Dynamics* **37**, 1039–1063.

Panagiotidou, A. I., Gazetas, G., and Gerolymos, N. [2012] "Pushover and seismic response of foundations on stiff clay: analysis with P-Δ Effects," *Earthquake Spectra* **28**(6).

Paolucci, R. [1997] "Simplified evaluation of earthquake induced permanent displacements of shallow foundations," *Journal of Earthquake Engineering* **1**, 563–579.

Paolucci, R., Shirato, M., and Yilmaz, M. T. [2008] "Seismic behavior of shallow foundations: shaking table experiments vs. numerical modeling," *Earthquake Engineering and Structural Dynamics* **37**(4), 577–595.

Pecker, A. [2003] "A seismic foundation design process, lessons learned from two major projects: the Vasco de Gama and the Rion Antirion bridges," *ACI International Conference on Seismic Bridge Design and Retrofit*, University of California at San Diego, La Jolla, California.

Pender, M. [2007] "Seismic design and performance of surface foundations," *4th International Conference on Earthquake Geotechnical Engineering*, Thessaloniki, Greece (CD-ROM).

Pitilakis, D. and Makris, N. [2010] "Dimensional analysis of inelastic systems with soil-structures interaction," *Bulletin of Earthquake Engineering* **8**, 1497–1514.

Raychowdhury, P. and Hutchinson, T. [2009] "Performance evaluation of a nonlinear Winkler-based shallow foundation model using centrifuge test results," *Earthquake Engineering and Structural Dynamics* **38**(5), 679–698.

Shakal, A., Haddadi, H., Graizer, V., Lin, K., and Huang, M. [2006] "Some key features of the strong motion data from the M 6.0 Parkfield, California, Earthquake of 28 September 2004," *Bulletin of the Seismological Society of America* **96**(4B), S90–S118.

Tassoulas, J. L. [1984] "An investigation of the effect of rigid sidewalls on the response of embedded circular foundations to obliquely-incident SV and P waves," in *Proc. of the International Symposium on Dynamic Soil–Structure Interaction*, Minneapolis, 4–5 September 1984, A.A.Balkemal, Rotterdam, pp. 55–63.

Ticof, J. [1977] "Surface footings on sand under general planar loads," Ph.D. Thesis, Department of Civil Engineering, University of Southampton, U.K.

Ukritchon, B., Whittle, A. J., and Sloan, S. W. [1998] "Undrained limit analysis for combined loading of strip footings on clay," *Journal of Geotechnical and Geoenvironmetal Engineering, ASCE* **124**(3), 265–276.

Vassiliou, M. F. and Makris, N. [2011] "Analysis of the rocking response of rigid blocks standing free on a seismically isolated base," *Earthquake Engineering and Structural Dynamics* **41**(2), 177–196.

Veletsos, A. S. and Nair, V. V. [1975] "Seismic interaction of structures on hysteretic foundations," *Journal of Structural Engineering, ASCE* **101**(1), 109–129.

Vesic, A. S. [1973] "Analysis of ultimate loads of shallow foundations," *Journal of Soil Mechanics Foundation Division, ASCE* **99**, 45–73.

Wong, H. L. and Luco, J. E. [1985] "Tables of impedance functions for square foundations on layered media," *Soil Dynamics and Earthquake Engineering* **4**, 64–81.

Yim, C. S., Chopra, A. K., and Penzien. J. [1980] "Rocking response of rigid blocks to earthquakes," *Earthquake Engineering and Structural Dynamics* **8**(6), 565–587.

Zhang, J. and Makris, N. [2001] "Rocking response of free-standing blocks under cycloidal pulses," *Journal of Engineering Mechanics* **127**(5), 473–483.